HHS Public Access

Author manuscript

Nat Neurosci. Author manuscript; available in PMC 2010 July 01.

Published in final edited form as:

Nat Neurosci. 2010 January ; 13(1): 120–126. doi:10.1038/nn.2453.

Evaluating self-generated decisions in frontal pole cortex of monkeys

Satoshi Tsujimoto[1,2], **Aldo Genovesio**[1,3], and **Steven P. Wise**[1]

[1]Laboratory of Systems Neuroscience National Institute of Mental Health National Institutes of Health 49 Convent Dr., Bethesda, Maryland 20892-4401

[2]Developmental Cognitive Neuroscience Laboratory Graduate School of Human Development and Environment Kobe University 3-11 Tsurukabuto, Nada-Ku, Kobe 657-8501, Japan

[3]Department of Physiology and Pharmacology Sapienza University of Rome 00185 Rome, Italy

Abstract

The frontal pole cortex (FPC) expanded dramatically during human evolution, but its function remains uncertain in either monkeys or humans. Here we report the first study of single-cell activity in this area. On every trial, monkeys decided between two response targets based on a 'stay' or 'shift' cue. Feedback followed at a fixed delay. FPC cells encoded the monkeys' decisions, not when they were made, but later, as feedback approached. This finding indicates a role for FPC in monitoring or evaluating decisions. A control task, which used delayed feedback, suggested that decision coding lasted until feedback only when the monkeys combined working memory with sensory cues to "self-generate" decisions, as opposed to when they simply followed trial-by-trial instructions. A role in monitoring or evaluating self-generated decisions could account for FPC's expansion during human evolution.

Keywords

Decision-making; monitoring; frontopolar cortex; area 10; anterior prefrontal cortex; prefrontal cortex

INTRODUCTION

The most anterior part of the cerebral cortex — area 10[1] or frontal pole cortex (FPC)[2, 3] — is the largest area in the prefrontal cortex of humans[4], one that expanded disproportionately during human evolution[5]. FPC has reciprocal connections with most prefrontal areas[6-9], and its cells have an unusually high density and number of dendritic spines[10]. These properties suggest that FPC plays a pivotal role in prefrontal function.

Corresponding author: Correspondence should be addressed to S.T. (tsujimoto@ruby.kobe-u.ac.jp) .

Author contributions S.T. and S.P.W. conceived and designed the experiment. S.T. and A.G. performed the experiment and analyzed the data. S.T., A.G. and S.P.W. wrote the paper.

The anterior prefrontal cortex, including FPC, has been implicated in several cognitive functions: establishing task sets[11]; prospectively coding and deferring goals[12-14]; making preconscious and exploratory decisions[15, 16]; detecting both actual and potential outcomes of decisions[17, 18]; coordinating internal and external influences on cognition[19]; combining results from multiple cognitive operations[2]; processing relational complexity[20, 21]; evaluating self-generated knowledge[22]; making evaluative judgments[23]; and detecting or employing deception[24, 25], among others. Some of these functions can be attributed to nearby areas rather than to FPC *per se*, but a clear-cut understanding of FPC function remains elusive nevertheless.

Single-cell neurophysiology could provide insight into FPC function, but an overlying bony air sinus limits access to this area in macaque monkeys. Recently, we overcame this problem[26], and here we report the neuronal activity that occurred as monkeys performed a strategy task[27-29]. This task incorporated two factors thought to be important in FPC function: coordinating internal and external sources of information[19] and combining cognitive processes to guide behavior[2]. We found that FPC neurons encoded decisions at feedback time.

Results

Behavior

We operantly conditioned two rhesus monkeys to perform an instructed strategy task (Fig. 1a). Each trial required the monkey to decide on one of two targets for a saccade.

A trial began when three stimuli appeared on a video screen: a fixation point (white circle) flanked by two saccade targets (white squares). After the monkey fixated the circle for 1.5 s, a cue instructed either a 'stay' or 'shift' decision. 'Stay' cues required a saccade to the same target chosen on the preceding trial; 'shift' cues required a saccade to the alternative target. In the *visually cued strategy task*, one of four randomly chosen visual stimuli appeared on each trial. A white vertical bar and a yellow square instructed 'stay', whereas a white horizontal bar and a purple square instructed 'shift' (Fig. 1b). In the *fluid-cued strategy task*, presented in a separate block of trials, one drop of fluid instructed 'stay', and two half-drops instructed 'shift' (Fig. 1b). Fluid delivery began at the start of the cue period. In both tasks, provided that the monkey maintained central fixation throughout the cue period (0.5 s) and the delay period (1.0, 1.25, or 1.5 s, randomly selected on each trial), the fixation point disappeared as the "go" signal, triggering a saccade to one (and only one) of the two targets. When the monkey acquired fixation on a target, both squares filled in. After a pre-feedback fixation period (0.5 or 1.0 s, in blocks of trials), feedback arrived in one of two forms: fluid reward for correct decisions or red squares over both targets for errors. After errors, the cue from that trial repeated on correction trials, which continued until the monkey performed correctly.

Both monkeys performed the visually cued strategy task at better than 90% correct (Suppl. Table 1). In the fluid-cued strategy task, the performance of the first monkey nearly matched this level, and the second monkey also performed above chance level (Suppl. Table 1).

Reaction times were ~310 ms (Suppl. Table 2), and both monkeys maintained fixation within ±1° on more than 90% of the trials.

Except where noted, the analyses reported here excluded both error and correction trials. In what follows, we describe our results in terms of the monkey's decisions. Although we did not design this experiment to distinguish decisions from spatial targets, saccade direction, actions, or responses, results on error trials helped us make this distinction.

FPC activity during the visually cued strategy task

We recorded neuronal activity in three tasks, two delay conditions, and two monkeys (Suppl. Table 3). For the visually cued strategy task, this database included 577 FPC cells: 347 from the first monkey, 230 from the second. A comparison of discharge rates during the fixation, cue, delay, and feedback periods (Kruskal-Wallis test, $\alpha = 0.05$) revealed 274 cells (47%) with significant task-related activity.

We tested each task-related cell for decision selectivity (left vs. right) and strategy selectivity (shift vs. stay) by two-way ANOVA, separately for each task period (Fig. 2). A typical cell with decision selectivity showed increased activity just before and after feedback, but only when the monkey had chosen one of the two targets (Fig. 2a and Suppl. Fig. 1). The frequency of cells preferring the left and right targets did not differ significantly (χ^2 test, $\chi^2 = 2.46$, $p = 0.12$; 62 left; 38 right).

Of the 274 task-related cells, 100 (36%) showed decision selectivity during the feedback period (Fig. 3). In no other task period did the percentage of decision-selective cells exceed chance level (Fig. 3a). With few and weak exceptions (Suppl. Fig. 2), task-related cells that lacked significant decision selectivity also showed activity modulation only during the feedback period. Decision selectivity occurred in both the 300-ms period before feedback and in the 200-ms period after the onset of feedback, with individual neurons showing various combinations (Fig. 3b). Strategy selectivity did not occur above chance level in any task period (Fig. 3a), and FPC cells also failed to encode either cue features or the decision made on the previous trial.

Measures of population activity confirmed the single-cell results. First, we computed the mean discharge rate for decision-selective cells. Both standard population averages (Fig. 2b) and *z*-score normalized averages (Suppl. Fig. 3) showed that FPC began to discriminate preferred vs. anti-preferred decisions ~0.5 s before feedback, a difference that persisted until ~0.5 s after the onset of feedback. The difference in activity between the preferred and anti-preferred decisions served as a measure of decision selectivity (Fig. 2c). Second, we quantified the strength of decision selectivity using ROC analysis. ROC values reflect the ability to decode a signal based on activity during a single trial, without being affected by a cell's overall activity level or its dynamic range, at the level of single cells (Fig. 2d) or the population mean (Fig. 2c). The mean ROC value during the feedback period was 0.69 ± 0.10 (s.d.), which significantly exceeded that for shuffled data (0.55 ± 0.01, Mann-Whitney U-test, $p<0.001$).

Error trials

Three separate statistical tests indicated less robust decision coding on error trials, compared to correctly performed trials (Fig. 4). We performed this analysis at the population level because the relatively small number of error trials precluded a cell-by-cell analysis. First, for preferred decisions, the mean firing rate on correct trials significantly exceeded that on error trials (Fig. 4a-c), for the overall feedback period (*t*-test, $t_{4775} = 3.20$, p = 0.0014), as well as for both its pre-feedback ($t_{4775} = 3.25$, p = 0.0012) and post-feedback ($t_{4775} = 2.70$, p = 0.007) components. Second, we performed a bootstrap analysis by shuffling the decision designation (left or right) and recalculating decision selectivity 1,000 times. For correct trials, the observed value vastly exceeded all 1,000 sets of shuffled data (Fig. 4d and Suppl. Fig. 4). In contrast, for error trials, the observed value fell within the range of shuffled data. Third, ROC analysis confirmed weaker decision selectivity during error trials (Fig. 4e).

Although all three analyses revealed weaker decision coding on error trials, they yielded inconsistent results on its statistical significance. The mean firing rates (Figs. 4a–c) did not significantly differ on error trials for preferred vs. anti-preferred decisions, either for the entire feedback period ($t_{911} = 1.78$, p = 0.08) or for its pre-feedback ($t_{911} = 1.69$, p = 0.09) or post-feedback ($t_{911} = 1.51$, p = 0.13) components. The bootstrap analysis (Fig. 4d) yielded a significant difference on error trials for the whole feedback period (p = 0.027, two-tailed test), but not for either the pre-feedback (p = 0.10) or post-feedback (p = 0.14) periods, separately (Suppl. Fig. 4). ROC analysis indicated significant decision coding on error trials during the pre-feedback period, but not during the post-feedback period (Fig. 4e).

Effects of delayed feedback

A control condition examined whether decision selectivity developed in relation to the time of the saccade or the time of feedback (Fig. 5). In the *standard condition*, described above, feedback arrived 0.5 s after the saccade. In separate blocks of trials, called the *delayed-feedback condition*, feedback occurred 1.0 s after the saccade. Feedback-period activity was assessed as before, from 300 ms prior to feedback onset until 200 ms afterward.

Of 65 task-related cells tested in the delayed-feedback condition, 21 cells (32%) had significant decision selectivity during the feedback period. The percentage did not differ significantly from the 36% observed in the standard delay condition (χ^2 test, $\chi^2 = 0.4$, p = 0.53). Thus, delaying feedback did not decrease the proportion of cells encoding the decision, and population analysis confirmed this result. In both the standard (Fig. 2b) and delayed-feedback (Fig. 5a) conditions, decision selectivity increased near the time of the saccade and persisted until after feedback, declining thereafter with a similar time-course (Fig. 5b). Note that had the signal followed a post-saccadic time course, the decay rate observed in the standard condition would have led to a loss of decision coding by the time feedback arrived in the delayed-feedback condition (Fig. 5c). ROC analysis confirmed the results from population activity averages (Suppl. Fig. 5).

Reward-as-feedback vs. reward *per se*

Because the activity modulation in FPC occurred around the time of reward and was greater for rewarded (correct) than for unrewarded (error) trials, we tested whether the activity

reflected reward delivery *per se*. In the fluid-cued strategy task, fluid was delivered to the monkey both as the cue and, later, as feedback (Fig. 1b). When presented as a cue, the fluid also served as a reward for maintaining fixation until cue onset. Hence, if the FPC cells anticipated or responded to reward *per se*, then they should have shown significant activity modulation both early and late in a trial.

We tested 302 neurons in the fluid-cued task, 194 and 108 cells from the first and second monkey, respectively. Of this population, 143 cells (47%) showed task-related activity, and 47 of the task-related cells (33%) showed decision selectivity (Fig. 3c and Suppl. Table 3).

During the fluid-cued strategy task, the activity of FPC cells (Fig. 6a) resembled the population averages (Fig. 6b) and ROC values (Fig. 6c). In contrast to the results expected for cells related to reward *per se*, FPC cells did not show significant activity modulation early in the trial, either before or after the fluid cue. As in the visually cued strategy task, significant activity modulation occurred only around feedback time. Cue-period activity was minimal and did not differ significantly between the visually cued and fluid-cued tasks (*t*-test, $t_{413} = 0.35$, $p = 0.73$), like pre-cue ($t_{413} = 0.31$, $p = 0.76$) and delay-period activity ($t_{413} = 0.50$, $p = 0.62$). These findings show that FPC activity did not reflect the anticipation or receipt of fluid rewards *per se*.

Results from the visually cued and fluid-cued tasks were similar in all other respects, as well. The feedback-period decision signal (Fig. 6d) did not differ between the two tasks in either timing (Kolmogorov-Smirnov test, $p = 0.26$) or magnitude (*t*-test, $t_{145} = 1.48$, $p = 0.14$), and only the feedback-period had higher than chance levels of decision selectivity (Fig. 3a,c). Similar to the visually cued task, the mean ROC value during the feedback period was 0.72 ± 0.12 (s.d.), which significantly exceeded the shuffled value of 0.57 ± 0.01 (Mann-Whitney U-test, $p<<0.001$).

Strategy vs. delayed-response task

To make a decision in the strategy task, the monkey had to remember its previous decision and combine this information with a visual cue. As a control, the *delayed-response task* eliminated these requirements: On each trial, a visuospatial cue (inside the left or right target) guided responses without reference to any previous trial (Fig. 7a). The time-course of events matched the visually cued strategy task. One version of the delayed-response task had the *standard*, 0.5 s delay between the saccade and feedback, another had *delayed* feedback (1.0 s).

Of 83 task-related cells recorded in this task, 22 (27%) showed decision selectivity during the feedback period (Fig. 7b). Mean task-related activity did not differ significantly between the visually cued strategy task and the delayed-response task (*t*-test, $t_{353} = -0.67$, $p = 0.50$ for the fixation period; $t_{353} = -0.86$, $p = 0.39$ for the cue period; $t_{353} = -0.59$, $p = 0.55$ for the delay period; $t_{353} = -0.98$, $p = 0.33$ for the feedback period).

We compared decision coding in the delayed-feedback condition to the standard-delay condition. The additional delay in feedback had no effect on decision selectivity for the strategy task, but it had a large and significant effect for the delayed-response task (Fig. 7c):

only 3 of 34 task-related cells (9%) showed decision selectivity with longer delays, which differed significantly from the strategy task (χ^2 test, $\chi^2 = 6.70$, $p<0.01$). Of 21 cells with decision selectivity in the delayed-feedback condition of the visually cued strategy task, we tested 8 in the delayed-response task. For this population, decision selectivity decreased significantly earlier in the delayed-response task than in the strategy task (Kolmogorov-Smirnov test, $p<0.001$), falling to the null level by the time feedback arrived (Fig. 7d).

Localization

The recordings came mainly from area 10, which we recognized by the close correspondence of its cytoarchitecture with the archetype of homotypical neocortex.

Despite the fact that we placed the recording chamber more laterally in the second monkey, the results from the two monkeys did not differ notably (Fig. 8). For example, both monkeys had nearly the same proportion of task-related neurons (Suppl. Table 3) and neurons with decision selectivity (χ^2 test, $\chi^2 = 0.98$, $p = 0.32$).

Discussion

FPC cells had remarkably simple properties. They encoded only the monkey's decision, and they did so only around feedback time. Most of the remaining task-related cells also showed activity modulation only around feedback time, but lacked decision selectivity. The relative simplicity of FPC's activity contrasts with the complexity of activity patterns in other prefrontal areas, which have activity related to sensory cues, working memory of previous goals, prospective memory for future goals, and problem-solving strategies, among a long list of cognitive functions[30]. FPC cells do not have any of these properties.

Three sets of findings inform and constrain our interpretation of FPC activity: timing, relationship with reward and trial outcome, and persistence for self-generated decisions. These topics are taken up, in turn.

Timing

FPC cells encoded the monkey's decision from the time of the saccade until ~0.5 s after the onset of feedback, whether feedback arrived at a standard 0.5-s delay or a prolonged 1.0-s delay (Fig. 5b). The decision signal thus had peri-feedback timing, rather than an exclusively post-movement time course. Although the strategy task required that the monkeys remember their previous decision, the fact that FPC's decision signal dissipated ~0.5 s after feedback indicates that other areas must have maintained this information over the intertrial interval, not FPC.

A decision signal around feedback time suggests that FPC provides other brain areas, particularly other prefrontal ones[6, 8], with the information needed to monitor the monkey's most recent decision. The FPC projects to orbitofrontal cortex[7], for example, and might send it decision information for the computation of expected, earned reward[31] and for assigning credit to decisions that produced a good outcome. Other prefrontal areas might use the same information for making the next decision. FPC's signal could also function in spatially selective top-down attention, which likely ramps up around feedback time, when monkeys

must attend to their decision and its outcome. Along the same lines, the supplementary eye field and the anterior cingulate cortex also have signals that monitor performance[32], and these areas, too, might influence or be influenced by FPC. Further studies should compare and contrast monitoring signals among these areas.

Reward and trial outcome

FPC cells did not encode the anticipation or delivery of fluid reward when it served as a strategy cue (Fig. 6), thus ruling out interpretations of FPC activity in terms of reward prediction or responses to rewards. The observation that FPC cells did not anticipate or respond to rewards when they were cues means that the pre- and post-reward activity seen later in the trial reflected the feedback conveyed by the fluid rather than its rewarding or reinforcing properties.

Although FPC's decision signal had nothing to do with rewards *per se*, it was much more robust on correct trials than on error trials (Fig. 4). Perhaps this result indicates that FPC cells encoded both the monkey's decision and a successful trial outcome. This view, along with the observation that the difference between correct and error trials preceded feedback (Fig. 4b), might suggest that FPC encoded a prospective aspect of monitoring, such as 'confidence'[33, 34]. Taken at face value, the prediction of outcome could serve a useful function. 'Confidence' in an upcoming, earned reward could contribute to the computations performed in areas such as orbitofrontal cortex, as noted above.

Another possibility, which we prefer, is that the stronger decision coding on correct trials indicates that FPC plays a role in monitoring decisions rather than actions, and that it monitors certain kinds of decisions. The actions taken on error trials, along with its spatial targets, saccade metrics, and related motor factors, did not differ from those on correct trials. But FPC activity differed significantly. The monitoring functions of FPC therefore probably relate to decisions, not to spatial or motor factors. Furthermore, these monitoring functions likely involve decisions made in the context of correct task performance rather than decisions taken in other contexts. For example, if the monkey had forgotten its previous decision, the random decisions that followed would have been errors half of the time. In such circumstances, and whenever there was noise in the decision-making mechanism[35], a weaker decision-monitoring signal would be expected.

Self-generation

One of our findings pointed to the importance of self-generational factors in FPC activity. In the delayed-response task, the location of a visual cue—alone—dictated the monkeys' response on each trial (Fig. 7a). This control task thus lacked two key requirements of the strategy task: (1) to remember the previous decision (or response location) and (2) to combine that memory with a sensory cue ('stay' or 'shift'). The combination of memories with sensory cues thus required monkeys to self-generate decisions, as opposed to simply following sensory instructions that dictated each response. In the delayed-feedback condition, the FPC's decision signal lasted until feedback arrived in the strategy task, but it did not do so in the delayed-response task (Fig. 7c,d). This result suggests that when decisions involve an element of self-generation, FPC's signal lasts until feedback time and

otherwise dissipates. Alternative accounts, such as attentional effects reflecting differences in task difficulty, cannot be ruled out entirely. However, no other aspect of activity differed between the strategy and delayed-response tasks, and the behavioral data did not indicate that the monkeys found the delayed-response task to be easier than the strategy tasks (Suppl. Tables 1 and 2).

Nevertheless, FPC did encode decisions in the delayed-response task (Fig. 7b). Because both monkeys had more than a year's experience with strategy tasks before we introduced the delayed-response task, this property could reflect the habit of monitoring decisions even when unnecessary. On this view, the decision signal was generated habitually but persisted only when necessary (Fig. 7c,d). Future recordings from monkeys trained only on the delayed-response task can clarify this issue.

Comparison with human FPC

Despite reasonable evidence that the FPC of rhesus monkeys, area 10, is homologous with at least part of the like-named area in humans, more evidence is needed, especially regarding connectivity in humans. In both species, the FPC has a homotypical cytoarchitecture that is generic even by the standards of such areas. In both species, the FPC has a similar location relative to other prefrontal areas, such as the orbitofrontal cortex and the medial agranular cortex. And, of course, both occupy the frontal pole. But the FPC in humans is much larger than in monkeys, and it may have additions or subdivisions that monkeys lack[4]. These differences, among others, limit the applicability of our results to the human FPC, but we can note some apparent similarities.

Our results point to a role for the monkey FPC in monitoring decisions, and some neuroimaging research in humans supports this idea, especially for medial FPC[36-38]. Selected neuroimaging research also accords with the idea that self-reference plays an important role in FPC function. According to one study, the anterior prefrontal cortex plays a role in evaluating self-generated decisions[22], but the area activated lies lateral and posterior to the FPC as construed here. More often, self-referential functions are ascribed to medial frontal areas[3, 19, 39-43]. For example, these areas are differentially activated when cues instruct a change in task, much like the 'shift' cue in our experiment, rather than when cues instruct a specific task[44]. These findings tie in with the participation of medial FPC in the "default-mode network"[45], and in both self-generation and self-reference, more generally. Based on its connections, the monkey FPC appears to lie within a "medial network"[7], which suggests that the monkey FPC could correspond to the medial FPC in humans.

Interpretational limitations and conclusions

We compared a nonspatially instructed strategy task with a spatially cued delayed-response task, using just two pre-reward delay periods. To test our conclusions, future studies should use an instructed-delay task with nonspatial stimuli and more delays.

Although we cited some selected neuroimaging results above, others are more difficult to reconcile with our findings. We might have predicted that self-generated rules would cause more FPC activation than instructed rules, but in a recent experiment they do not[46].

Similarly, prospective coding is considered a key function of FPC[12], but FPC cells showed no prospective coding of future goals or strategies. Perhaps FPC functions only in particular aspects of prospection. One neuroimaging study indicates that medial FPC activity reflects left-right decisions[16], like our result, but that signal occurs long before the subject's movement, whereas ours followed movement. Outcome-related signals occur in Pavlovian conditioning[17], which requires neither decisions nor actions. These signals could reflect a monitoring process that occurs automatically, even in the absence of decisions or actions. Anterior prefrontal cortex shows activity related to task set[11], [47] and rules[48], a finding that appears at odds with the absence of strategy-related activity in our data. Here, the precise location of neuroimaging activations might be a critical factor. The areas activated with new task sets and rules are situated laterally in the anterior cortex and either correspond to lateral parts of FPC (area 10) or anterior parts of dorsolateral prefrontal cortex (area 46 or 47). If the monkey FPC corresponds to the medial FPC of humans, then the absence of such set- or rule-related activity in our results should not be surprising. Finally, although we discuss our result in terms of evaluating the affirmative decision to chose one of the two targets, the decision-selective signal could just as well reflect an evaluation of the choice not made.[18] Experiments comparing FPC activity during Pavlovian and instrumental tasks, tasks with more than two choices, and tasks with changing outcome probabilities should help resolve these issues.

In conclusion, the present findings point to a role of FPC in monitoring and evaluating decisions, especially those with a self-generational component. These functions could account for the dramatic expansion of FPC during human evolution[5]. Our results are also compatible with the idea that FPC coordinates external and internal contributions to cognition[19] and combines the products of separate cognitive operations[2], in this case involving sensory cues and memories. The combination of cognitive operations across different domains of knowledge could provide a key source of human creativity[49].

Methods

Subjects and recording procedures

Two male rhesus monkeys (*Macaca mulatta*) were studied, weighing 10.0 kg and 10.7 kg, respectively. During task performance, each monkey sat in a primate chair with its head fixed facing a video screen 32 cm away. Initial fixation was constrained within ± 3° and target fixation within ± 3.75°. All procedures accorded with the *Guide for the Care and Use of Laboratory Animals* and were approved by the NIMH Animal Care and Use Committee.

Details of procedures for FPC recordings, including surgical procedures and chamber designs, were described previously[26]. Briefly, using aseptic techniques and isofluorane anesthesia (1%–3%, to effect), a recording chamber (10.65 mm inner diameter) was implanted over the exposed dura mater of the right FPC.

Single-cell activity was recorded from PF using up to 16 platinum-iridium electrodes (0.5–1.5 MΩ at 1 KHz) inserted into the cortex with a multi-electrode drive (Thomas Recording, Giessen, Germany). Single-cell potentials were isolated offline using a cluster cutting

technique (Off Line Sorter, Plexon, Dallas, Texas). An infrared oculometer (Arrington Research, Inc., Scottsdale, AZ) recorded eye position.

The two versions of the strategy task and the delayed-response task had the same time-course, and the pre-feedback delay never varied across tasks within a day. For the standard delay condition, blocks in the visually cued strategy task averaged 130–140 trials (139 ± 45 trials, s.d., in monkey 1, 131 ± 35 trials in monkey 2); blocks in the fluid cued strategy task averaged ~100 trials (97 ± 31 trials in monkey 1, 101 ± 20 trials in monkey 2); and blocks in the delayed-response task averaged ~70 trials (74 ± 21 trials in monkey 1, 66 ± 16 trials in monkey 2). For the delayed-feedback condition, blocks in the visually cued strategy task averaged ~140 trials (140 ± 32 trials in monkey 1, 143 ± 34 trials in monkey 2); and blocks in the delayed-response task averaged 60-100 trials (99 ± 15 trials in monkey 1, 60 ± 12 trials in monkey 2). During the recording of neuronal activity, the task blocks were usually presented in an ABAAB order, where A represents the strategy task and B represents the delayed-response task. Most often, the first of these blocks began prior to the initiation of recording, as several neurons were isolated with multiple electrodes, and this first block was extended as necessary to collect ~140 trials of neuronal data.

Stimulus material

The central, filled white circle had a diameter of 0.6° (visual angle); the two unfilled white target squares measured 2° × 2° and appeared 11.6° from the center of the video screen. The square strategy cues measured 2° × 2°, and the rectangular cues were 5° × 1°. The filled, red squares used as negative feedback had the same dimensions as the target squares. In the delayed-response task, the filled white circles used as visuospatial cues appeared in the center of the target square (Fig. 7a) and had a diameter of 0.6°.

Reward volume

A regulated liquid-delivery device[50] ensured that the volume of fluid (0.2 ml) given as a reward at the end of a successful trial matched the amount delivered as a cue in the fluid-cued strategy task, for both the single drop and the two half-drops (0.1 ml each) of fluid (Fig. 1b).

Data analysis

To identify task-related neurons, we used the Kruskal-Wallis test ($\alpha = 0.05$) to compare mean firing rate among four task periods: the fixation period (0.5 – 1.0 s after fixation onset), the cue period (0.08 – 0.50 s after cue onset), the delay period (0.0 – 1.0 s after delay onset), and the feedback period (from 0.3 s before feedback onset until 0.2 s afterward). If this test yielded a significant effect of task period, then a neuron was classified as task related. For task-related neurons, we then used a two-factor ANOVA ($\alpha = 0.05$) separately for each task period, with factors decision (left vs. right) and strategy (stay vs. shift). Although many task-related cells showed neither effect, they modulated their activity at the same time as those that did, during the feedback period. A few cells (Suppl. Fig. 2), however, showed some weak modulation during the cue or delay period. This weak modulation was not selective for the decision or strategy. Of 577 cells tested in the visually cued strategy task, 14 (2%) showed increase in activity during the cue period like the cell in

Suppl. Fig. 2a, and 38 (7%) showed decrease in activity during the delay period like the cell in Suppl. Fig. 2b, among some similar minorities. These percentages are near those expected by chance.

For the population averages, we measured the mean firing rate of each neuron in 20-ms bins aligned on cue and reward onset. To confirm these results, we also calculated the normalized population averages, based on the *z*-score of each bin's firing rate relative to the mean activity from 1.0 s before cue onset to 0.5 s after reward onset. Two-sample Kolmogorov-Smirnov tests ($\alpha = 0.05$) examined the timing differences between pairs of conditions. There were 21 bins for the cue period (since a 420-ms period was analyzed) and 25 bins for the feedback period. The results were similar when we analyzed a larger time-window, one that encompassed the entire durations illustrated in the figures.

For the ROC (receiver operating characteristic) analysis, we computed the area under the ROC curve to measure decision selectivity, with 0.5 indicating no selectivity and 1.0 corresponding to maximal selectivity. To test whether the ROC values exceeded those expected by chance, a bootstrap analysis was performed. For each neuron, we shuffled the decision designation for each trial and recalculated the ROC values. This process was repeated 1,000 times for each neuron, and shuffled ROC values were compared to observed values (Mann-Whitney U-test, $\alpha = 0.05$). The time-course of decision selectivity was examined by calculating the area under ROC curve in a 200-ms time window that stepped across the trial in increments of 20 ms.

In addition to *t*-tests, a bootstrap procedure was used to compare decision selectivity in correct and error trials (Fig. 4d and Suppl. Fig. 4). In correct trials, the decision designation (left or right) was shuffled randomly. Then, the "preferred" and "anti-preferred" decision was determined as in the conventional analysis, and their difference calculated. Finally, for error trials, the decision designation was similarly shuffled, and the same "preferred" and "anti-preferred" decisions were applied and their difference calculated. This shuffling procedure was repeated for 1,000 times, which yielded 1,000 sets of activity differences for correct and error trials.

Histology

The recording sites were reconstructed by standard histological analysis and MRI. After 10 days, the animal was deeply anesthetized and then perfused with 10% (v/v) formol saline, with a pin inserted through the center of the recoding chamber immediately prior to and during the perfusion. Frozen, coronal sections were Nissl stained with cresyl violet.

Our recordings extended through most of the mediolateral extent of the monkey FPC, and decision-selective cells were dispersed fairly evenly among the recording sites (Fig. 8). We did not observe any differences in properties along the mediolateral dimension of the FPC, although our recordings were limited to a small area (a 5-mm diameter for each monkey), with a caudomedial bias in the first monkey and a rostrolateral bias in the second. The FPC recordings came from dorsomedial part of area 10 of Walker[1]. In all cases, the recording sites were within 5 mm of the most rostral extent of layer 4. We made no attempt to determine the laminar distribution of recording sites.

Supplementary Material

Refer to Web version on PubMed Central for supplementary material.

Acknowledgements

We thank Drs. Silvia Bunge, Giuseppe di Pellegrino, Elisabeth Murray, Richard Passingham, Narender Ramnani, and Peter Rudebeck for comments on drafts of this paper. Dr. Andrew Mitz, Mr. James Fellows, and Ms. Ping Yu provided technical support. This work was supported by the Division of Intramural Research of the National Institute of Mental Health (Z01MH-01092) and by a Grant-in-Aid for Scientific Research on Innovative Areas (21119513) from the Ministry of Education, Culture, Sports, Science and Technology, Japan. S.T. was supported by a research fellowship from the Japan Society for the Promotion of Science.

Reference List

1. Walker AE. A cytoarchitectual study of the prefrontal areas of the macaque monkey. J. Comp. Neurol. 1940; 73:59–86.
2. Ramnani N, Owen AM. Anterior prefrontal cortex: Insights into function from anatomy and neuroimaging. Nat. Rev. Neurosci. 2004; 5:184–194. [PubMed: 14976518]
3. Burgess, PW.; Simons, JS.; Dumontheil, I.; Gilbert, SJ. The gateway hypothesis of rostral prefrontal cortex (area 10) function. In: Duncan, J.; McLeod, P.; Phillips, L., editors. Measuring the mind: Speed, control, and age. Oxford University Press; Oxford: 2009. p. 215-246.
4. Öngür D, Ferry AT, Price JL. Architectonic subdivision of the human orbital and medial prefrontal cortex. J. Comp. Neurol. 2003; 460:425–449. [PubMed: 12692859]
5. Semendeferi K, Armstrong E, Schleicher A, Zilles K, Van Hoesen GW. Prefrontal cortex in humans and apes: A comparative study of area 10. Am. J. Phys. Anthropol. 2001; 114:224–241. [PubMed: 11241188]
6. Jones EG, Powell TPS. An anatomical study of converging sensory pathways within the cerebral cortex of the monkey. Brain. 1970; 93:793–820. [PubMed: 4992433]
7. Carmichael ST, Price JL. Connectional networks within the orbital and medial prefrontal cortex of macaque monkeys. J. Comp. Neurol. 1996; 371:179–207. [PubMed: 8835726]
8. Petrides M, Pandya DN. Efferent association pathways from the rostral prefrontal cortex in the macaque monkey. J. Neurosci. 2007; 27:11573–11586. [PubMed: 17959800]
9. Hagmann P, et al. Mapping the structural core of human cerebral cortex. PLoS. Biol. 2008; 6:e159. [PubMed: 18597554]
10. Jacobs B, et al. Regional dendritic and spine variation in human cerebral cortex: A quantitative Golgi study. Cereb. Cortex. 2001; 11:558–571. [PubMed: 11375917]
11. Sakai K. Task set and prefrontal cortex. Annu. Rev. Neurosci. 2008; 31:219–245. [PubMed: 18558854]
12. Okuda J, et al. Differential involvement of regions of rostral prefrontal cortex (Brodmann area 10) in time- and event-based prospective memory. Int. J. Psychophysiol. 2007; 64:233–246. [PubMed: 17126435]
13. McClure SM, Ericson KM, Laibson DI, Loewenstein G, Cohen JD. Time discounting for primary rewards. J. Neurosci. 2007; 27:5796–5804. [PubMed: 17522323]
14. Koechlin E, Basso G, Pietrini P, Panzer S, Grafman J. The role of the anterior prefrontal cortex in human cognition. Nature. 1999; 399:148–151. [PubMed: 10335843]
15. Daw ND, O'Doherty JP, Dayan P, Seymour B, Dolan RJ. Cortical substrates for exploratory decisions in humans. Nature. 2006; 441:876–879. [PubMed: 16778890]
16. Soon CS, Brass M, Heinze HJ, Haynes JD. Unconscious determinants of free decisions in the human brain. Nat. Neurosci. 2008; 11:543–545. [PubMed: 18408715]
17. Ramnani N, Elliott R, Athwal BS, Passingham RE. Prediction error for free monetary reward in the human prefrontal cortex. Neuroimage. 2004; 23:777–786. [PubMed: 15528079]

18. Boorman ED, Behrens TEJ, Woolrich MW, Rushworth MFS. How green is the grass on the other side? Frontopolar cortex and the evidence in favor of alternative courses of action. Neuron. 2009; 62:733–743. [PubMed: 19524531]
19. Burgess PW, Dumontheil I, Gilbert SJ. The gateway hypothesis of rostral prefrontal cortex (area 10) function. Trends Cogn. Sci. 2007; 11:290–298. [PubMed: 17548231]
20. Kroger JK, et al. Recruitment of anterior dorsolateral prefrontal cortex in human reasoning: A parametric study of relational complexity. Cereb. Cortex. 2002; 12:477–485. [PubMed: 11950765]
21. Bunge SA, Helskog EH, Wendelken C. Left, but not right, rostrolateral prefrontal cortex meets a stringent test of the relational integration hypothesis. Neuroimage. 2009; 46:338–342. [PubMed: 19457362]
22. Christoff K, Ream JM, Geddes LP, Gabrieli JD. Evaluating self-generated information: Anterior prefrontal contributions to human cognition. Behav. Neurosci. 2003; 117:1161–1168. [PubMed: 14674837]
23. Zysset S, Huber O, Ferstl E, von Cramon DY. The anterior frontomedian cortex and evaluative judgment: An fMRI study. Neuroimage. 2002; 15:983–991. [PubMed: 11906238]
24. Ganis G, Kosslyn SM, Stose S, Thompson WL, Yurgelun-Todd DA. Neural correlates of different types of deception: An fMRI investigation. Cereb. Cortex. 2003; 13:830–836. [PubMed: 12853369]
25. Karim AA, et al. The truth about lying: Inhibition of the anterior prefrontal cortex improves deceptive behavior. Cereb. Cortex. 2009 PMID: 19443622.
26. Mitz AR, Tsujimoto S, Maclarty AJ, Wise SP. A method for recording single-cell activity in the frontal-pole cortex of macaque monkeys. J. Neurosci. Methods. 2009; 177:60–66. [PubMed: 18977387]
27. Genovesio A, Brasted PJ, Mitz AR, Wise SP. Prefrontal cortex activity related to abstract response strategies. Neuron. 2005; 47:307–320. [PubMed: 16039571]
28. Genovesio A, Brasted PJ, Wise SP. Representation of future and previous spatial goals by separate neural populations in prefrontal cortex. J. Neurosci. 2006; 26:7281–7292. [PubMed: 16822986]
29. Tsujimoto S, Genovesio A, Wise SP. Transient neuronal correlations underlying goal selection and maintenance in prefrontal cortex. Cereb. Cortex. 2008; 18:2748–2761. [PubMed: 18359779]
30. Wise SP. Forward frontal fields: Phylogeny and fundamental function. Trends Neurosci. 2008; 31:599–608. [PubMed: 18835649]
31. Pochon JB, et al. The neural system that bridges reward and cognition in humans: An fMRI study. Proc. Natl. Acad. Sci. U.S.A. 2002; 99:5669–5674. [PubMed: 11960021]
32. Schall JD, Stuphorn V, Brown JW. Monitoring and control of action by the frontal lobes. Neuron. 2002; 36:309–322. [PubMed: 12383784]
33. Kiani R, Shadlen MN. Representation of confidence associated with a decision by neurons in the parietal cortex. Science. 2009; 324:759–764. [PubMed: 19423820]
34. Kepecs A, Uchida N, Zariwala HA, Mainen ZF. Neural correlates, computation and behavioural impact of decision confidence. Nature. 2008; 455:227–231. [PubMed: 18690210]
35. Genovesio A, Tsujimoto S, Wise SP. Encoding problem-solving strategies in prefrontal cortex: Activity during strategic errors. Eur. J. Neurosci. 2008; 27:984–990. [PubMed: 18279367]
36. van Duijvenvoorde ACK, Zanolie K, Rombouts SA, Raijmakers ME, Crone EA. Evaluating the negative or valuing the positive? Neural mechanisms supporting feedback-based learning across development. J. Neurosci. 2008; 28:9495–9503. [PubMed: 18799681]
37. Walsh ND, Phillips ML. Interacting outcome retrieval, anticipation, and feedback processes in the human brain. Cereb. Cortex. 2009 PMID: 19429861.
38. Lawrence NS, Jollant F, O'Daly O, Zelaya F, Phillips ML. Distinct roles of prefrontal cortical subregions in the Iowa gambling task. Cereb. Cortex. 2009; 19:1134–1143. [PubMed: 18787233]
39. Burgess PW. Function and localization within rostral prefrontal cortex (area 10). Phil. Trans. Roy. Soc. Lond., Series B, Biol. Sci. 2007; 362:887–899.
40. Gilbert SJ, et al. Functional specialization within rostral prefrontal cortex (area 10): a meta-analysis. J. Cogn. Neurosci. 2006; 18:932–948. [PubMed: 16839301]

41. Mason MF, et al. Wandering minds: The default network and stimulus-independent thought. Science. 2007; 315:393–395. [PubMed: 17234951]
42. Gusnard DA, Akbudak E, Shulman GL, Raichle ME. Medial prefrontal cortex and self-referential mental activity: Relation to a default mode of brain function. Proc. Natl. Acad. Sci. U.S.A. 2001; 98:4259–4264. [PubMed: 11259662]
43. Christoff K, Ream JM, Gabrieli JD. Neural basis of spontaneous thought processes. Cortex. 2004; 40:623–630. [PubMed: 15505972]
44. Forstmann BU, Brass M, Koch I, von Cramon DY. Internally generated and directly cued task sets: an investigation with fMRI. Neuropsychologia. 2005; 43:943–952. [PubMed: 15716164]
45. Raichle ME, et al. A default mode of brain function. Proc. Natl. Acad. Sci. U.S.A. 2001; 98:676–682. [PubMed: 11209064]
46. Bengtsson SL, Haynes JD, Sakai K, Buckley MJ, Passingham RE. The representation of abstract task rules in the human prefrontal cortex. Cereb. Cortex. 2009; 19:1929–1936. [PubMed: 19047573]
47. Sakai K, Passingham RE. Prefrontal set activity predicts rule-specific neural processing during subsequent cognitive performance. J. Neurosci. 2006; 26:1211–1218. [PubMed: 16436608]
48. Bunge SA. How we use rules to select actions: A review of evidence from cognitive neuroscience. Cogn. Affect. Behav. Neurosci. 2004; 4:564–579. [PubMed: 15849898]
49. Mithen, S. The Prehistory of the Mind. Thames and Hudson; London: 1996.
50. Mitz AR. A liquid-delivery device that provides precise reward control for neurophysiological and behavioral experiments. J. Neurosci. Methods. 2005; 148:19–25. [PubMed: 16168492]

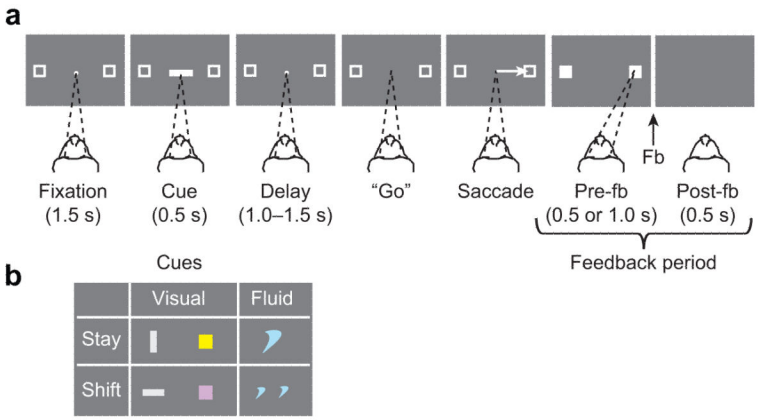

Figure 1.

Task and cues. (**a**) Sequence of task events. Gray rectangles: video screen; dashed lines: fixation target. A central white circle (the fixation point) and two unfilled white squares (not to scale) appeared first, followed by a cue (the white horizontal rectangle in this case) and a delay period. Offset of the fixation point served as the "go" signal for a saccade (white arrow) to one of the two squares. Feedback (Fb) arrived after the saccade. (**b**) Cues and the strategies each instructed. Blue shapes: drops of fluid.

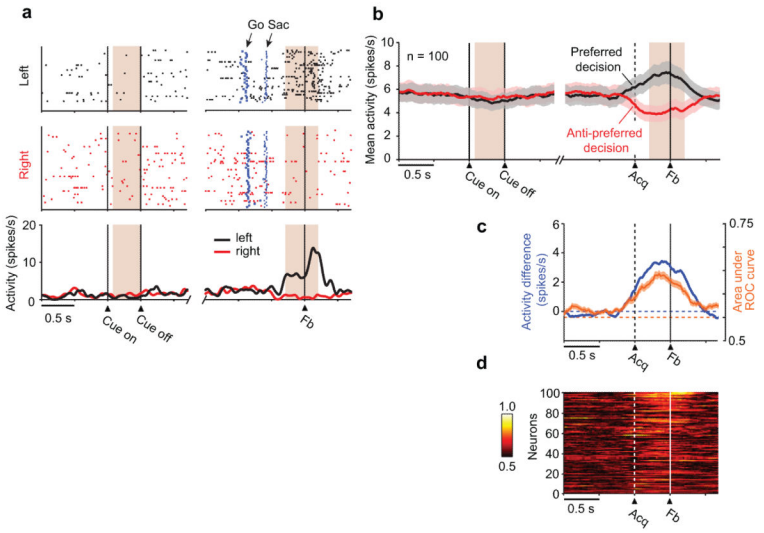

Figure 2.

Decision-selective activity in the visually cued strategy task. (**a**) Activity from a single cell aligned on cue onset (left), and feedback (Fb, right), with saccade onset (sac) and the "go" cue indicated by marks on each raster line, and cue offset (cue off) marked by a vertical line. Raster displays show spike times with spike-density averages below. Background shading: analyzed periods. Feedback-period activity for left decisions (8.2 ± 5.3 spikes/s, mean ± s.d.) significantly exceeded that for right decisions (0.8 ± 1.7 spikes/s; two-way ANOVA, $F_{1, 87} = 85.0$, $p<<0.001$). (**b**) Population activity for decision-selective FPC neurons, computed separately for each neuron's preferred (black) and anti-preferred (red) decision. Shading: s.e.m. Bin width: 20 ms, 3-bin moving average. Dashed vertical line: target acquisition (acq). (**c**) The activity difference between preferred and anti-preferred decisions (blue), from **b**, and the mean ROC value from **d** (orange, shading: s.e.m.) Dashed horizontal lines: blue, no activity difference; orange, mean of shuffled ROC values. (**d**) ROC plots for decision-selective FPC neurons, with the area under the ROC curve color-coded for each cell (scale at left), ranked according to values during the feedback period.

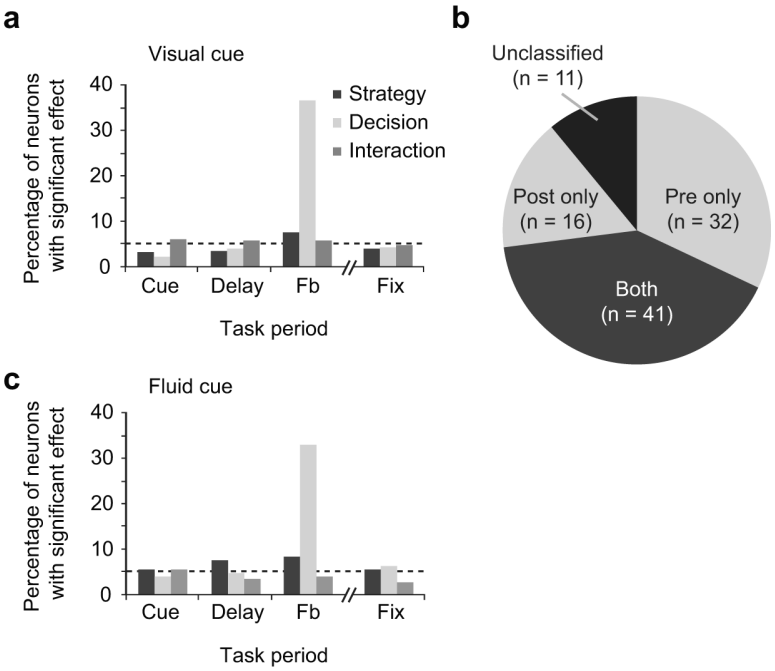

Figure 3.

Decision-selective activity by task period. (**a**) For the visually cued strategy task, FPC neurons with significant main or interaction effects (two-way ANOVA, factors: strategy and decision), as a percentage of task-related neurons (n = 274). Dashed line: percentage expected by chance. A significantly above-chance percentage of decision effects occurred only in the feedback (Fb) period (χ^2 test, $\chi^2 = 83.1$, $p<0.001$). Fix: pre-cue fixation period, ANOVA based on the strategy and decision factors from the previous trial. (**b**) Number of neurons that showed decision-selective activity during the 300-ms pre-feedback period (pre) and the 200-ms post-feedback period (post). Some neurons (unclassified) showed significant decision-selectivity for the 500-ms feedback period as a whole, but not for either its pre- or post-feedback components. (**c**) As in **a**, for the fluid-cued strategy task (n = 143). A significantly above-chance percentage of decision effects occurred only in the feedback period (χ^2 test, $\chi^2 = 36.3$, $p<0.001$).

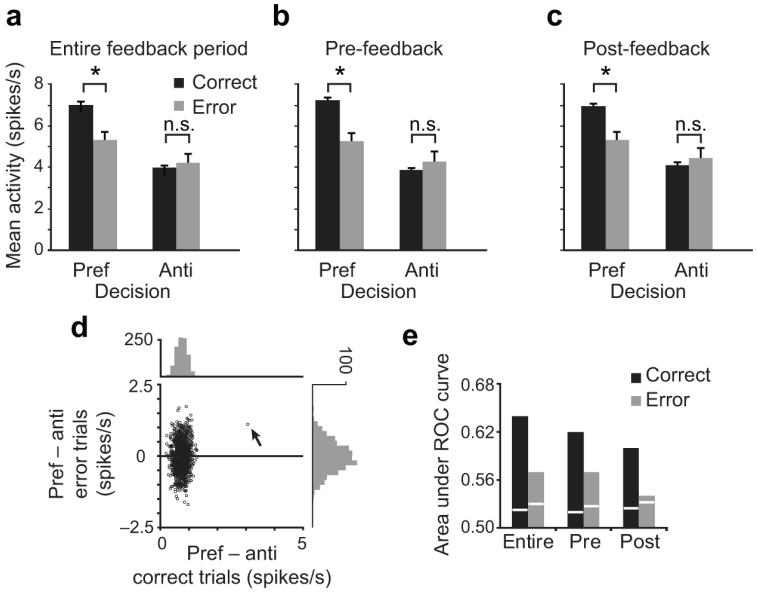

Figure 4.

Population activity on error trials. (**a**) Mean firing rate on correct and error trials, during the entire feedback period, for cells with decision-selective activity. Error bars : s.e.m. Pref: preferred decision; Anti: anti-preferred decision. Activity differed on correct vs. error trials for preferred (*, $p<0.001$) but not for anti-preferred decisions (n.s., not significant, *t*-test, $t_{4787} = 0.69$, $p = 0.49$). Activity also differed for preferred vs. anti-preferred decisions on correct trials (black bars, *t*-test, $t_{8495} = 14.99$, $p<0.001$). (**b**) As in **a**, for the 300-ms pre-feedback component of the feedback period ($t_{4829} = 0.99$, $p = 0.32$ for anti-preferred decisions; $t_{8495} = 14.94$, $p<0.001$ for preferred vs. anti-preferred decisions on correct trials); (**c**) As in **a**, for the 200-ms post-feedback component of the feedback period ($t_{4851} = 0.79$, $p = 0.43$ for anti-preferred decisions; $t_{8495} = 12.34$, $p<0.001$ for preferred vs. anti-preferred decisions on correct trials). (**d**) Activity difference between preferred and anti-preferred decisions for the observed (arrow) and shuffled data (remaining points): correct trials vs. error trials, for the entire feedback period. (**e**) Area under ROC curve for correct and error trials, for the entire feedback period, as well as for its pre-feedback (pre) and post-feedback (post) components. White lines: ROC values for shuffled data.

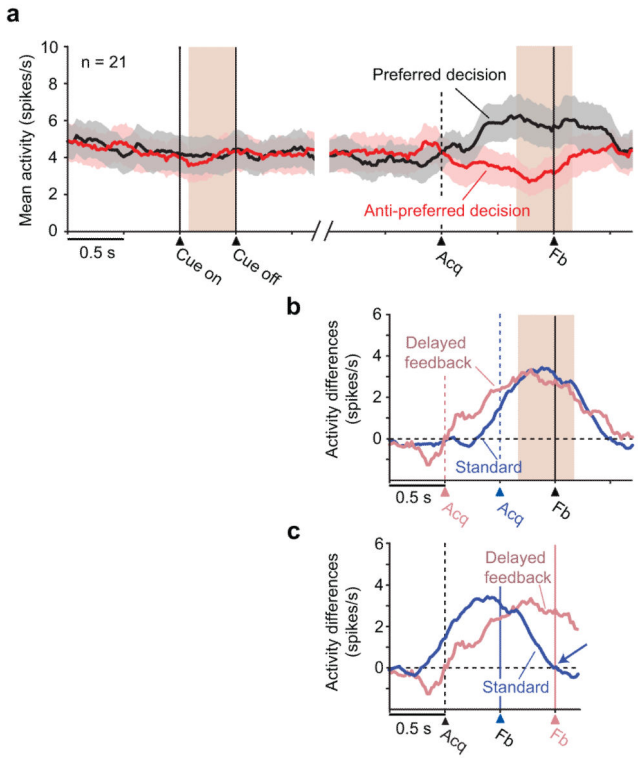

Figure 5.

Effect of delayed feedback. (**a**) FPC population activity when feedback arrived 1.0 s after target acquisition (acq). Format as in Fig. 2b. Shading: s.e.m. For FPC neurons with significant decision-selective activity during feedback period (n = 21). (**b**) Activity difference between preferred and anti-preferred decisions for the standard delay condition (blue, from Fig. 2b) and the delayed-feedback condition (pink, from **a**). Aligned on the onset of feedback (fb). (**c**) As in **b**, but aligned on target acquisition (acq). Note that with standard delays the activity difference decays to zero within 1.0 s of target acquisition (arrow), which is when feedback arrives in the delayed-feedback condition.

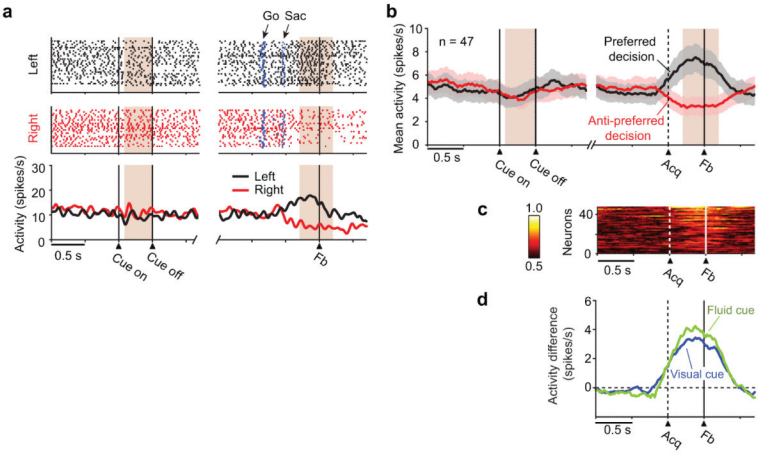

Figure 6.

Decision-selective activity in the fluid-cued strategy task. (**a**) Activity from an FPC neuron in the format of Fig. 2a. During the feedback period the cell showed 14.1 ± 5.1 spikes/s for preferred decisions vs. 5.4 ± 4.4 spikes/s for its anti-preferred decision (mean ± s.d.; two-way ANOVA, $F_{1, 57} = 48.0$, $p<<0.001$). (**b**) Population activity for FPC neurons having significant decision-selective activity during the feedback period in the fluid-cued strategy task (n = 47). Format as in Fig. 2b. (**c**) Sliding ROC plots for the same population as in **b**. Format as in Fig. 2d. (**d**) Activity difference between preferred and anti-preferred decisions in the visually cued strategy task (blue, from Fig. 2b) and in the fluid-cued strategy task (green, from **b**).

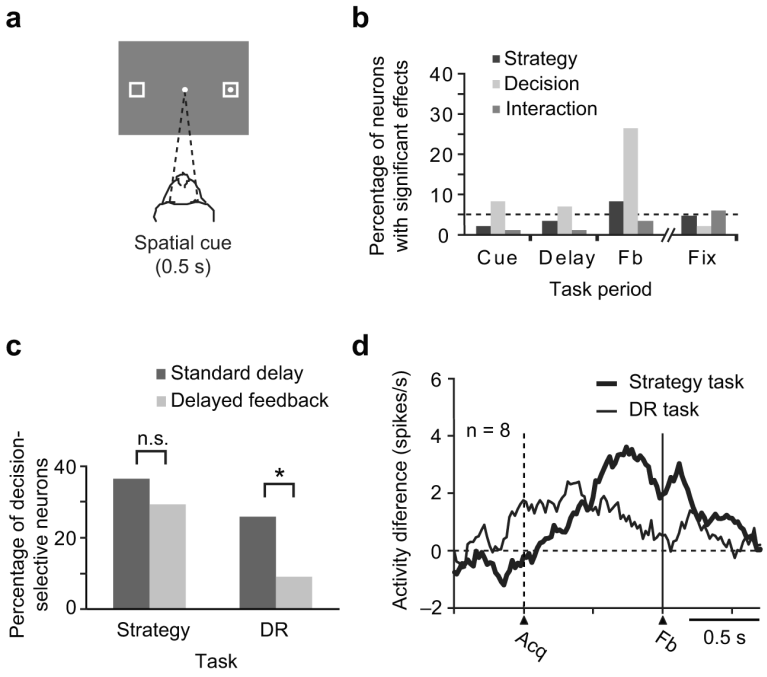

Figure 7.

Activity in the delayed-response task. (**a**) Example of a visuospatial cue in the delayed-response task. (**b**) Results of the two-way ANOVA. Format as in Fig. 3a. (**c**) Percentage of decision-selective neurons for the visually cued strategy task and the delayed-response (DR) task, for both the standard- and delayed-feedback conditions. In the delayed-response task, the percentage of decision-selective cells was significantly lower (*) in delayed-feedback condition than in the standard condition (χ^2 test, $\chi^2 = 4.49$, $p = 0.034$). In the visually cued strategy task, this difference was not statistically significant ($\chi^2 = 0.4$, $p = 0.53$). (**d**) Population averages for decision-selective neurons tested in the delayed-feedback condition: Activity difference between preferred and anti-preferred decisions in the visually cued strategy task (thick curve) vs. the delayed-response task (thin curve).

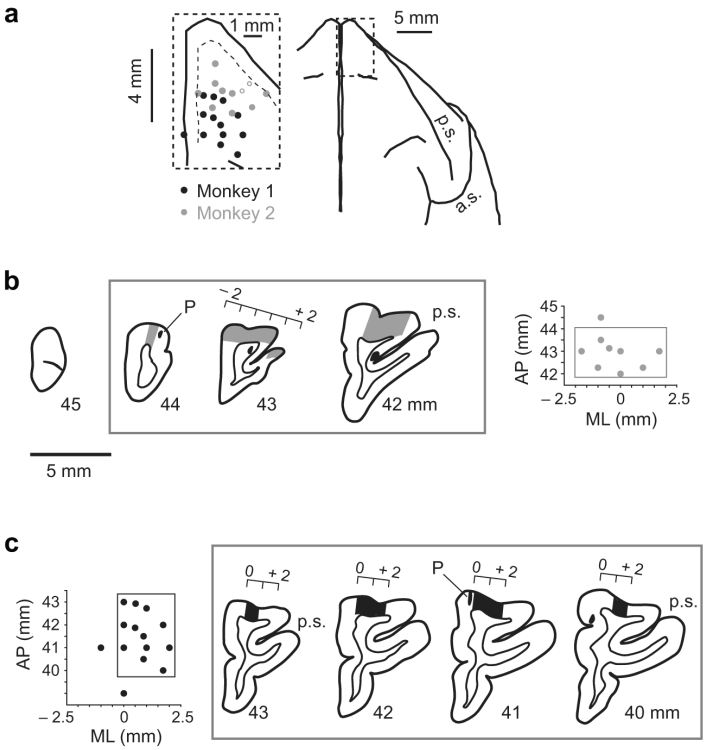

Figure 8.

Recording locations. (**a**) Penetration sites with decision-selective cells (filled circles) in the visually guided strategy task. Dorsal view of cerebral cortex: composite of two monkeys. a.s.: arcuate sulcus; p.s.: principal sulcus. The dashed box in the right part of the panel matches the dashed box to the left. Dashed line: layer 4. Each dot represents the site of an electrode array, which included four or more electrodes. Anterior is up. (**b**) Section drawings from the second monkey. Medial is left; dorsal is up. Thick lines: pial surface; thin lines: layer 6-white matter boundary. Filled spot: defect caused by pin (P), inserted at the center of the recording chamber. Coordinates relative to the interaural line (Horsley-Clarke AP0). The boxes around three of the sections (left) and the data points (right) bound the location of most cells with decision selectivity. Shading: recording locations. AP: anteroposterior axis; ML: mediolateral axis. (**c**) As in **b**, for the first monkey. Task-related cells in the fluid-cued strategy task and the delayed-response task were observed in nearly identical recording sites as those illustrated here.